Experimental investigation on the micro damage evolution of chemical corroded limestone subjected to cyclic loads

Hao Li [a,b], Dongmin Yang[a,*], Zuliang Zhong[b], Yong Sheng[a], Xinrong Liu[b]

[a] School of Civil Engineering, University of Leeds, Leeds, LS2 9JT, UK

[b] School of Civil Engineering, University of Chongqing, Chongqing, 400044, China

*corresponding author. Email address: D.Yang@leeds.ac.uk

Abstract

Micro damage evolution in chemical corroded limestone samples subjected to cyclic loads is investigated using Nuclear Magnetic Resonance (NMR) system. Based on the experimental data of Magnetic Resonance Imaging (MRI), T_2 values and porosity, the micro damage evolution process is visualized and analyzed. It is found that the porosity and micro cracking of the corroded limestone samples increase with the cyclic loading, and the micro damage evolution process consists of three distinct stages: micro crack emergence stage, micro damage development stage and damage development accelerated stage. Chemical erosion is found to have a significant influence on the propagation of micro cracks and accelerate the damage development of the limestone samples under cyclic loading. With the same number of load cycles, the chemical corroded samples always have lower peak strength than that of the water softened samples. Before the inflection point in the micro damage-loading cycles curve, the main damage is caused by new micro cracks increase inside the limestone; while after this point, the new micro crack emergence is being restrained, and the existed micro cracks connect into rupture bands. A damage model is finally proposed to quantify the damage evolution of the chemical corroded rocks subjected to cyclic loads.

Keywords: Nuclear Magnetic Resonance (NMR); T_2 spectrum distribution; Micro damage; Chemical erosion; Cyclic loading.

1 Introduction

Underground construction excavation, such as tunnel and nuclear waste deposition, *etc*., leads to the cyclic loads near the excavation surface and subsequent stress-induced instabilities [1, 2]. The instability and failure of engineering rocks is closely related to the initiation and propagation of micro cracks that are induced by cyclic loads [3]. Propagation of micro cracks inside rocks is determined by the external loads as well as the surrounding environment. Engineering rocks are always surrounded by water, which is a significant influential factor for the mechanical characteristics of rocks by reducing their strength and even causing geological disasters during the excavation processes [4, 5]. This is because that the surrounding water often contains chemical icons [6, 7], which can react with the mineral inside the rocks. Therefore, understanding the micro damage evolution of chemical

corroded engineering rocks under cyclic loading conditions is vital in order to reduce the risk of causing potential engineering disasters during excavation.

Over the past few years, considerable efforts have been made to investigate the mechanical response of intact rocks under cyclic loading. Results have shown that the fatigue properties of rock materials are dependent on the maximum stress, loading frequency and amplitude, *etc*. Based on energy dissipation, Liu *et al*. [8] established damage evolution equations for two typical rocks using the uniaxial cyclic loading test results, and proposed a new damage constitutive model to describe the behaviour of rocks under cyclic loading. The amended damage constitutive model can describe the degree of compactness of rocks accurately. Shayea [9] reported that the dynamic elastic modulus and Poisson's ratio increased with the confining pressure, and under cyclic loading their values during unloading were slightly higher than those during loading. Ray *et al*. [10] concluded that failure strength and elastic modulus of Chunar sandstone subjected to cyclic stress decreased with the increase of strain rate, and the uniaxial compressive strength decreased with the increase of loading cycles. Yoshinaka *et al*. [11-13] conducted cyclic loading tests to investigate the deformation behaviour of the soft rocks, including Kobe mudstone, sandstone, Ohya tuff and Yokohama siltstone, and introduced a procedure for strain correction, Young's modulus estimation and yield location. Bagde and Petros [14, 15] conducted cyclic loading tests on rock samples to investigate the relationship between loading amplitude and frequency and the fatigue strength and deformation behaviour. It was found that fatigue strength of the rock under dynamic cyclic loading is influenced by the micro structure of the rock samples, the Young's modulus decreases when increasing the cyclic loading frequency and amplitude, and there is no obvious relationship between the dynamic energy and the cyclic loading frequency. Sun *et al*. [16] carried out cyclic loading tests at multi-level amplitudes on sandstone samples to investigate the damage evolution law of the Chaboche and developed a multiaxial fatigue damage model for damage accumulation.

Meanwhile, a few studies investigated the influence of environment, such as cyclic temperature and freezing conditions, on the mechanical properties of rocks. Li *et al*. [17] conducted cyclic loading experiments to investigate the mechanical properties of a jointed rock mass under freezing and cyclic loading conditions, found that the original samples usually have a higher fatigue strength than the frozen and water saturated samples, and thus proposed a dynamic, fatigue damage model for cracked, frozen sandstones. Zhou *et al*. [18] conducted cyclic uniaxial stress-temperature tests on basalt rock specimens to investigate the deformation characteristics of the samples subjected to cyclic uniaxial stress and cyclic temperature. Results showed that the peak strain of damaged specimens undergoes initial, steady and acceleration stages; the Young′s modulus decreases rapidly in the initial cycles, but the declining rate decreases further in subsequent cycles. A damage model for rocks subjected only

to cyclic temperature was also proposed. Mahmutoglu [19] conducted several cyclic temperature tests on sandstones, and found that there is an obvious decrease in the mechanical properties of the sandstones after being treated with cyclic temperature.

Most studies of cyclically loaded rocks have focused on the changes of macro-mechanical properties. However, under the effect of different external loading conditions, great changes could take place inside the rock, such as micro-cracking [20, 21], which then cause the macro-mechanical degradation of the rock [22]. However, experimental studies on chemical corroded rocks subjected to cyclic loads are rarely reported, and the influence of cyclic loading coupled with chemical erosions on micro damage evolution of rock still remains unclear. The micro-cracking inside the rock can be investigated using computerized tomography (CT) technique [23-26] or Nuclear Magnetic Resonance (NMR) System [27-30]. NMR has been widely applied in medical diagnosis, geotechnical engineering and oil and gas exploration [31, 32]. It recently starts to be used in rock engineering for internal microstructure imaging and characterization [30].

In this study, NMR and cyclic loading tests are carried out to investigate the micro damage evolution of chemical corroded limestone samples subjected to cyclic loads. Through the analysis of the Magnetic Resonance Imaging (MRI) and T_2 values, the micro damage of the limestones has been visualized and calculated, and the relationship between peak strength degradation and micro damage is investigated. A damage model for rocks subjected to cyclic loads coupled with chemical erosion is established, which can be potentially used for predicting rock strength in practical design of underground constructions, slops and dams and roads in water surrounded regions.

2 Rock samples and experimental tests

2.1 Sample preparation

The rock samples are limestone, taken from Jinyun Mountain Tunnel in Chongqing China. The Jinyun Mountain Tunnel has two tunnels, each with a length of 7.379 km and have a maximum depth of 220 m. Limestone, a common sedimentary rock in southwest China and is the main rock of Jinyun Mountain, is selected as the test samples in this experiment. All the samples are drilled from a single block without macroscopic cracks and machined and finely ground into cylindrical shapes with a length of 100 mm and a diameter of 50 mm, as shown in Figure 1. According to the X-ray diffraction (XRD) analysis it is found that the limestone samples are composed of 92% calcspar and quartz and 1% accessory minerals. A typical microstructure of the limestone is shown in Figure 2.

Figure.1. Limestone samples

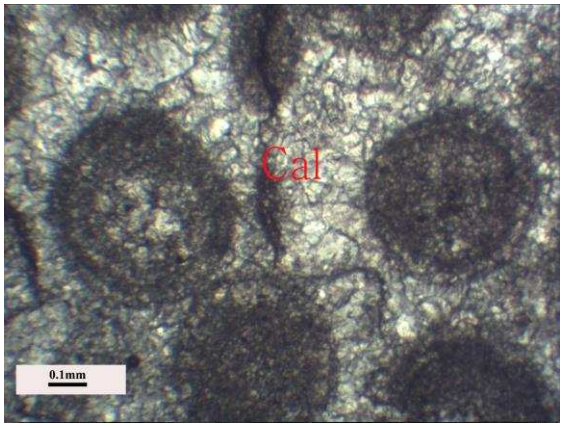

Figure.2. Microscope image of a limestone sample: Cal, calcspar.

2.2 Chemical solutions

According to water sample analysis, the water samples collected from the Jinyun tunnel construction site in Chongqing, has a pH value of 6.5 and the main icons are Na^+, Ca^{2+}, Mg^{2+}, SO_4^{2-}, Cl^- and HCO^-. To simplify the experimental study, the complex ionic compositions of the water are replaced by Na_2SO_4 solution, which is made by NaCl solution added with H_2SO_4. Three pH values (3, 5 and 7) of the Na_2SO_4 solution are used in the tests and the initial concentration of the chemical solutions is all 0.01 $mol \cdot L^{-1}$.

2.3 Test methodology and process

Figure.3 shows the NMR system, and a T_2 spectrum. The NMR system measures the signal intensity of hydrogen atoms, which depends on the number and size of pores inside the rock, in the fully-saturated rock and outputs transverse relaxation time distribution (T_2 spectrum), porosity and Magnetic Resonance Imaging (MRI), which can be used to investigate the pore size distribution and micro structure damage of the rock.

All the mechanical tests are conducted using the Rock Testing System, as shown in Figure 4.

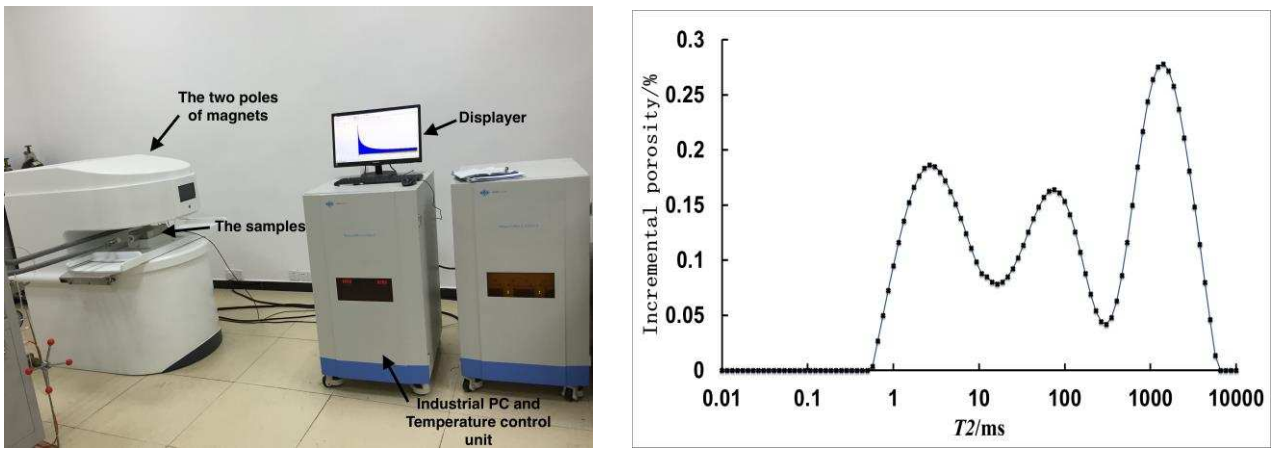

Figure.3. The NMR system and an example of its T_2 spectrum.

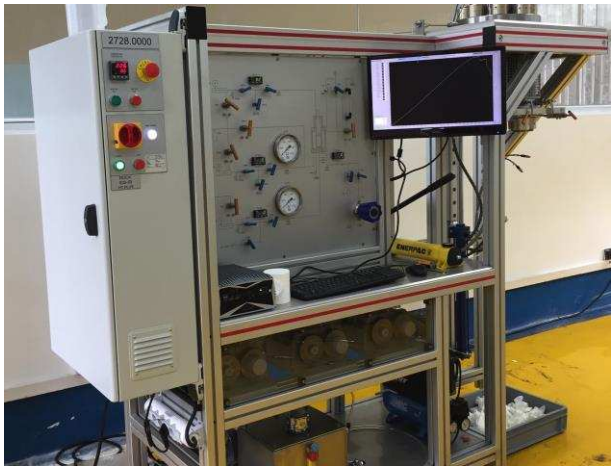

Figure.4. The Rock Testing System

The test process is as follows:

(1) The samples are saturated using a vacuum saturation device. After saturation for 24h, all the samples are warped with preservative film to prevent evaporation, and then putted into the test box of the NMR machine. With the help of the industrial computer of the NMR machine, the initial T_2 spectrum and the porosity of the limestone samples are obtained. After that, samples with similar initial porosity and T_2 spectrum distribution are selected for later experiments.

(2) The limestone samples are divided into four groups (Group A, Group B, Group C, Group D). Each group has 8 samples and they are immersed in pH3, pH5, pH7 Na_2SO_4 solutions and distilled water separately for 60 days.

(3) After reaching the designed erosion period, NMR tests are conducted to investigate the micro structure changes of the rock sample. After that, regular uniaxial compression tests are conducted to obtain the average uniaxial compression of the chemical corroded and water soft sample. Rock testing system, which is shown in Fig 4, is employed to complete the compression test. A total of four samples (each group is chosen one sample) are used for the uniaxial compression test, and the test result shows

the uniaxial compression strength (UCS) is 74.96 MPa (sample corroded by pH3 solution), 101.35MPa (sample corroded by pH5 solution), 119.09 MPa (sample corroded by pH7 solution), 134.89MPa (water soft sample).

(4) Cyclic loading tests are conducted at the same loading levels but with different cycle numbers. Each cycle of uniaxial cyclic loading processes is as follows: the rock sample is loaded to 85% of its UCS with loading rate of 0.01 mm/min. When the maximum load is reached, the stress of each sample is then unloaded to zero with the same rates. Each test consists of 8 cyclic loading stages, with 10 loading cycles, 20 loading cycles, 30 loading cycles, 40 loading cycles, 50 loading cycles, 60 loading cycles, 70 loading cycles, 80 loading cycles, respectively. These 8 stages are conducted on the corresponding 8 samples in a group. Take Group A as an example: sample A-1 is suffered from 10 times cyclic loads, sample A-2 is suffered from 20 times cyclic loads…. sample A-8 is suffered from 80 times cyclic loads. The load-time curves during the cyclic loading for the water soft limestone samples is shown in Fig 5 as an example.

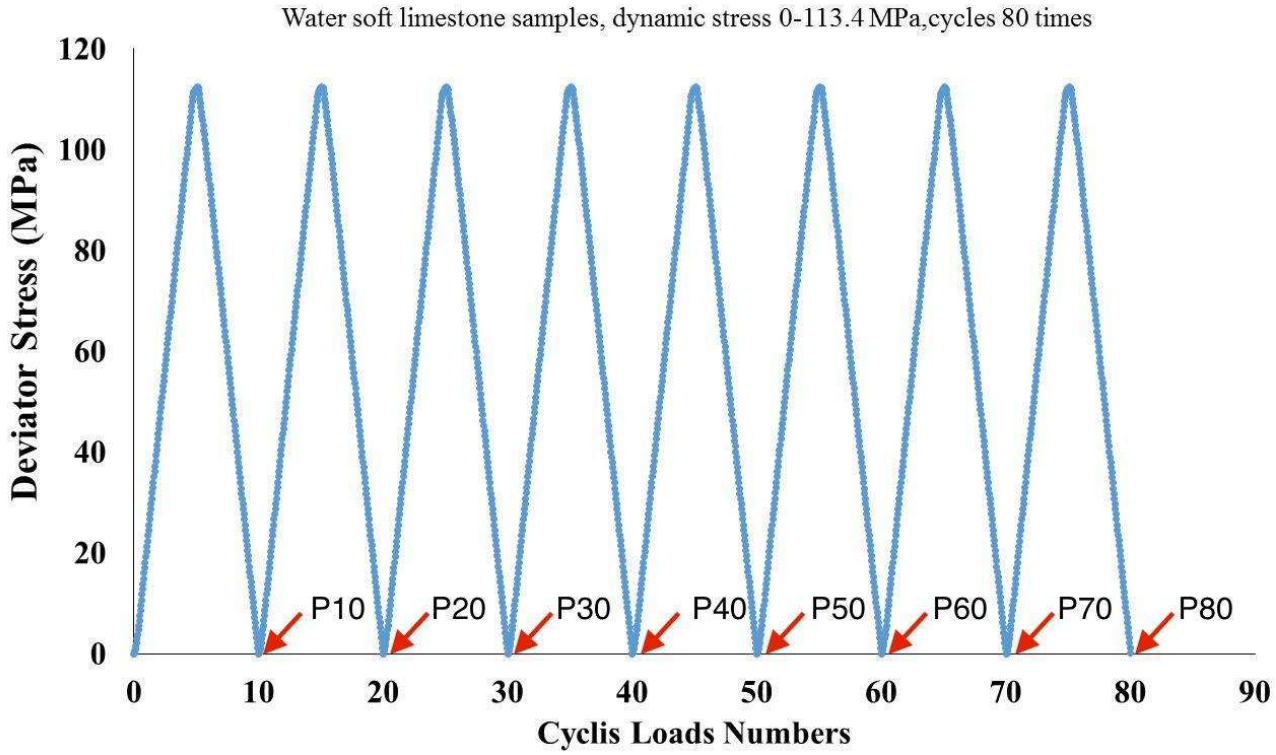

Fig .5. The load-time curves during the cyclic loading for the limestone samples

(5) When a sample reaches the designed number of cycles, it is taken for the NMR test to obtain the T_2 spectrum, porosity and MRI. After the NMR test, the limestone sample is taken out of the NMR machine and put into the pressure cell of the Rock 600-50 test system for compression test until it is completely ruptured.

3 Experimental results

3.1 T_2 spectrum distribution and MRI of the samples

Under the effect of cyclic loads, great changes including the micro damages could take place at micro scale within rocks, which can cause changes of the macro-mechanical behaviors. In addition, when coupled with chemical erosion, the relationship between micro damage and macro mechanical properties of the rocks becomes more complex. To further explore the rock damage evolution law under the cyclic loading, T_2 spectrum distribution and MRI, which is the inner section images of the chemical corroded samples treated with cyclic loading. MRI is taken only from the middle cross-section of the sample, thus they are mainly used to visualize the damage evolution trend of the samples under different loading cycles. While, the T_2 spectrum, which is obtained by testing the whole sample, can accurately reflect the microstructure changes in the whole sample after suffered different loading cycles and chemical erosion.

Combine all the data obtained from NMR, the evolution of micro damage in the chemical corroded limestones during the entire cyclic loading period can be investigated and analyzed. The NMR inner section images of the samples are shown in Fig.6.

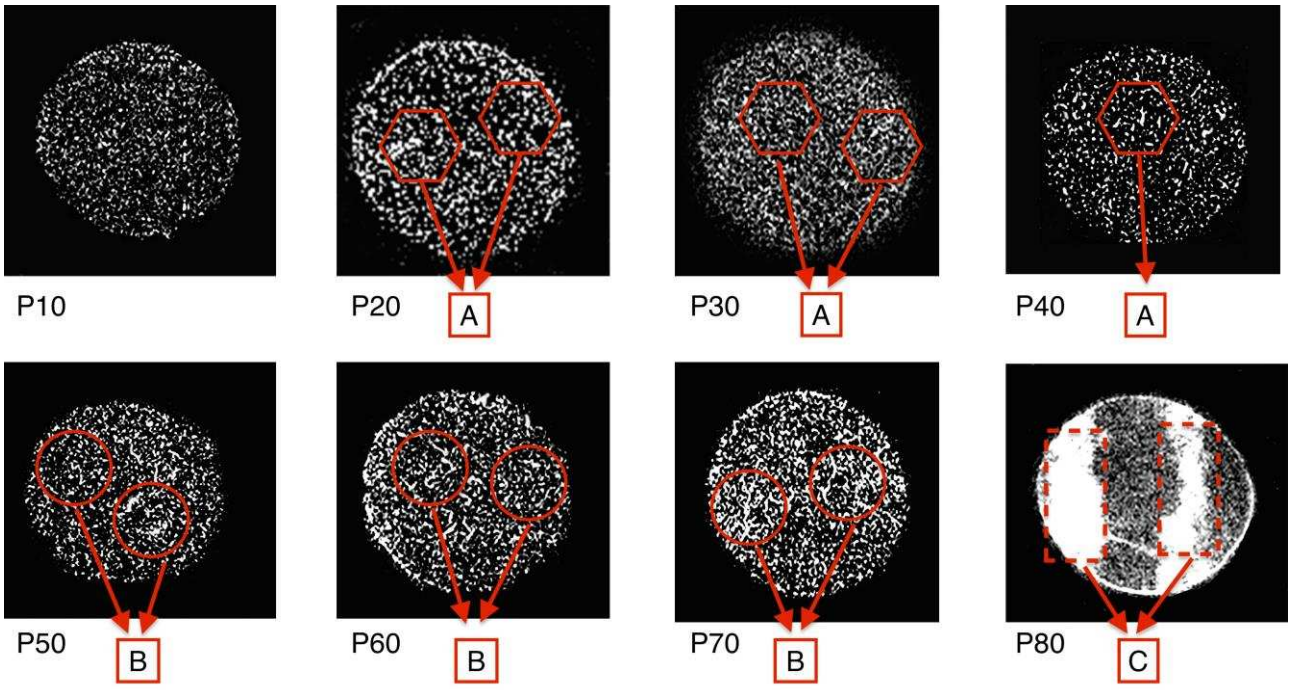

(a) Limestone samples immersed in pH3 solution

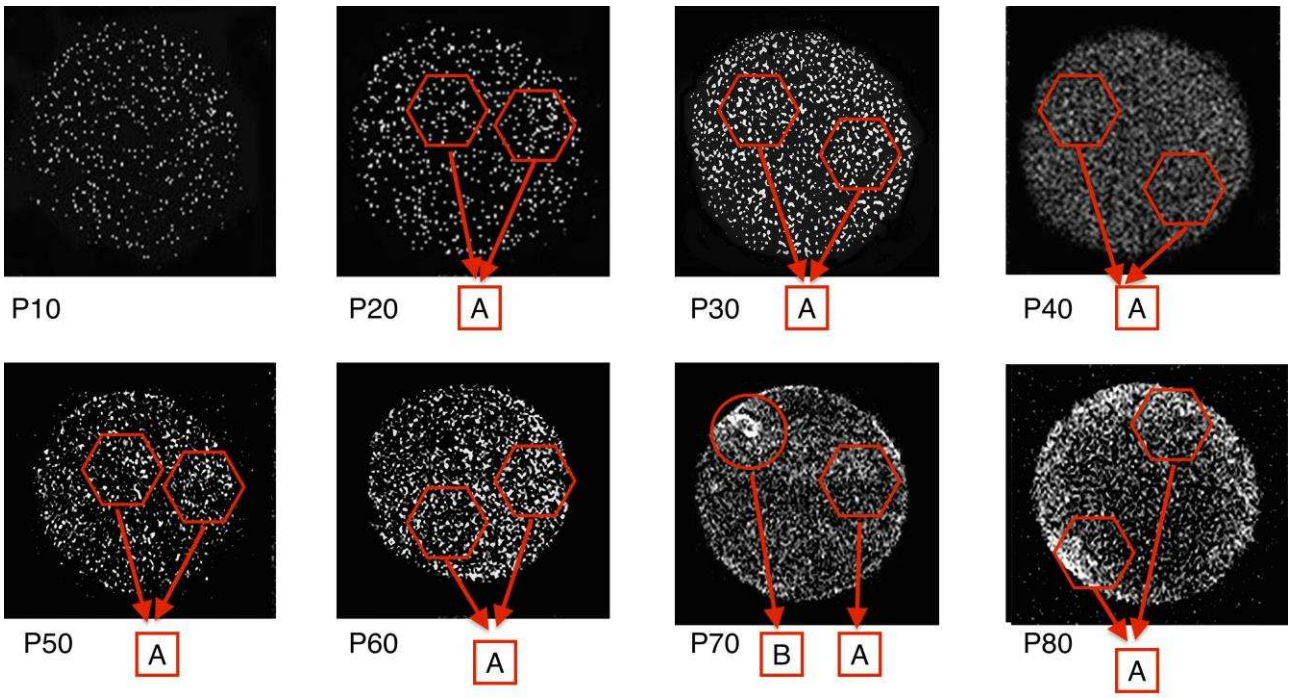

(b) Limestone samples immersed in distilled water

Fig .6. The NMR inner section images of the samples after cyclic loading. ('A' indicates smaller pores, 'B' indicates connection of pores into cracks and 'C' indicates the macro rupture.)

The bright areas in the images correspond to pores inside the limestone samples. An increase of the brightness and the number of white points indicates an increase of the porosity. It can be seen from Fig.6 that image brightness of the limestone samples increase as the increase of number of load cycles. While, the image of the water softened sample suffered 40 times of cyclic loads is blur and darker than other images in this group, this is due to the heterogeneous distribution of the porosity inside the rock. A quite significant increase of porosity occurs between the 10 times and 80 times of load cycles, where the brightness of the images increases sharply. And there are macro cracks emerged in the samples corroded by pH3 solution after 80 loading cycles, as shown in Fig 6 (a). In general, the brightness and the number of white points in the images of the chemical corroded samples is higher than that in distilled water, which confirms the micro damage of limestone in the chemical solutions develop faster than in distilled water.

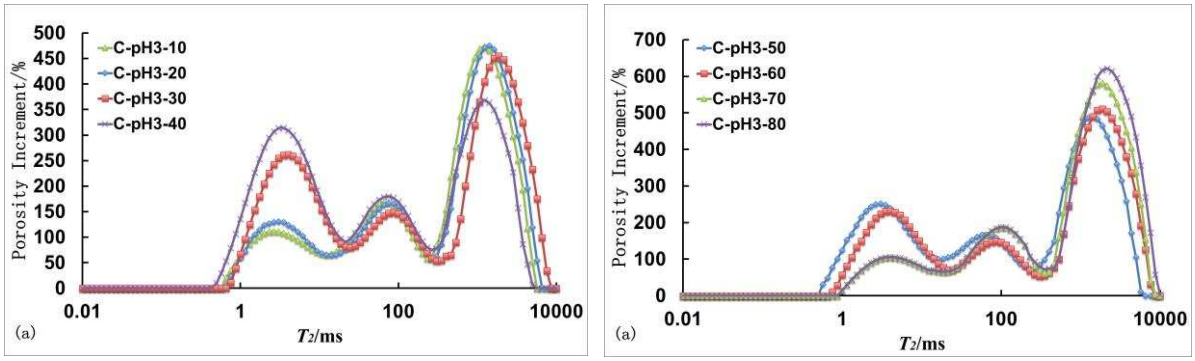

(a) Chemical corroded samples (PH=3)

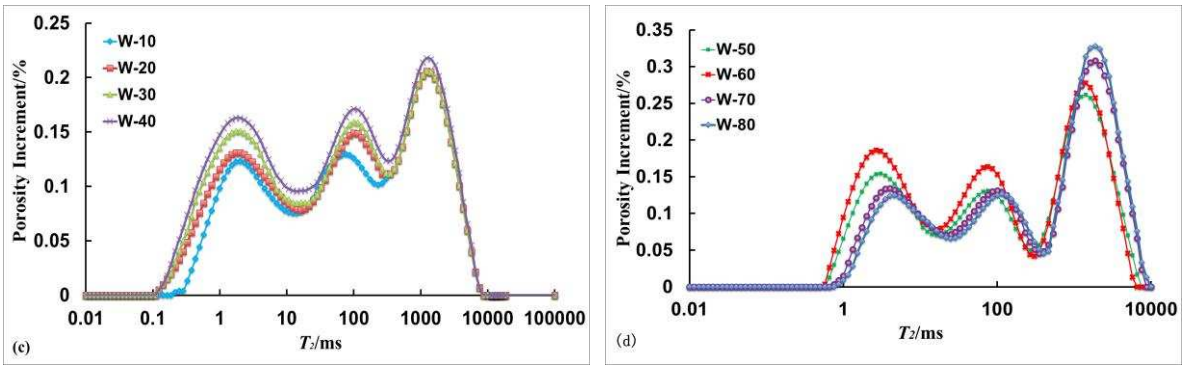

(b) Water soft samples

Fig.7. T_2 distributions of samples under cyclic loading conditions (Left: 10-40 cycles; Right: 50-80 cycles).

Fig. 7 shows the T_2 spectrum curves of the samples immersed in pH3 solution and distilled water from 10 cycles to 80 cycles. The T_2 spectrum curve is related to the porosity and pore size distribution of the rock, *i.e.*, the porosity increases with the T_2 spectrum area and the peak point of the curve increases when the pore size increase. The T_2 spectrum curves for limestone sample in this test have three peaks. The left and the middle peaks indicate the small pores and the right one indicates bigger pores. With more load cycles, the T_2 spectrum curve has shown higher peaks and changes in curve shape, which means there are changes in porosity.

A few observations can be made from the test results: (1) after cyclic loading, the area under the T_2 spectrum curves of the limestone samples have largely changed, indicating significant changes of microstructure of the limestone samples. (2) From Fig. 6 and Fig. 7, of the evolution of damage in the limestone samples (taking samples corroded by pH3 solution as an example) subjected to cyclic loads show three distinctive stages: micro crack emergence stage, micro damage development stage and damage acceleration stage. In the micro crack emergence stage, there is a slight increase of the first peak of the T_2 spectrum curve, which means there are newly emerged small pores inside the limestone samples. After 30 to 60 cycles, the limestone sample enters into the micro damage development stage, where the first and the second peaks of the T_2 spectrum curve increase greatly, which indicates the significant increase of porosity due to the emergency of new pores as well as the convergence of existing pores. This is then followed by the damage acceleration stage which leads to rupture. In this stage, the first and second peak decrease, while the third peak increases significantly, indicating the initiation of new micro cracks is constrained, and the internal cracks of the specimen are gradually converged and interconnected to form a shear band to cause the failure. (3) Compared to water soft ones, the chemical corroded limestone samples are more sensitive to the cyclic loading: the T_2 spectrum area and peak point growth of the samples corroded by pH3 solution are more faster

and obvious than the water corroded ones, that indicates the porosity and micro cracking increase of the chemical corroded samples are faster than that in distilled water.

3.2 Porosity

The porosity of corroded samples obtained by NMR is shown in Table 1, and the porosity increment-loading cycles curve is shown in Fig. 8.

Table 1 Porosity of corroded samples after cyclic loads

Chemical solution	Porosity before cyclic loading	Porosity after cyclic loading							
		10	20	30	40	50	60	70	80
pH3 Na_2SO_4	7.15	7.84	8.13	8.24	8.32	8.39	8.48	8.79	14.33
pH5 Na_2SO_4	6.44	7.03	7.21	7.33	7.42	7.47	7.58	7.78	8.12
pH7 Na_2SO_4	5.75	6.27	6.43	6.53	6.57	6.64	6.74	6.86	6.96
Distilled water	5.22	5.67	5.81	5.86	5.89	5.93	5.97	6.02	6.05

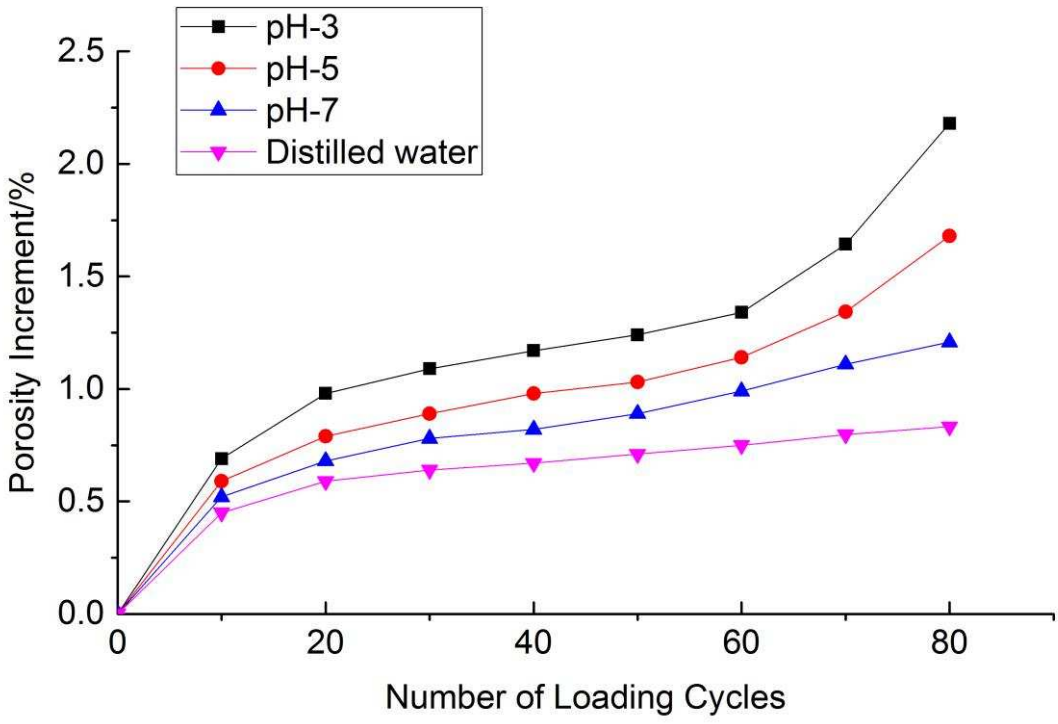

Fig. 8 Porosity increment rate vs number of loading cycles

It can be found that the porosity of the limestone samples increase with the increasing loading cycles, which means the micro damage of the samples increase continuously. The porosity increment of limestone samples corroded by pH3 solution are always greater than that in other pH values solution, and develop faster than other group of samples. Due to the chemical ions exchange between the solution and the rock [23], there is a slight increase of porosity of the samples corroded by pH7 solution, and the porosity growth is higher than that in distilled water, which porosity increment is smallest among all the sample groups.

4 Damage model of corroded limestone under cyclic loading

4.1 Damage induced by cyclic loading and chemical erosion

Damage leads to the changes of mechanical properties of rocks, *e.g*. the elastic modulus, hardness, strength and strain, *etc*. [33, 20]. In order to quantify the influence of damage on the mechanical properties of rock, usually a damage variable must be defined and a fatigue cumulative damage model must be established. The methods to define the damage variable vary, and the damage variable could be elastic modulus, energy dissipation, maximum strain, residual strain or ultrasonic wave velocity, *etc.* [34]. No matter what kind of variable is used, the damage evolution law must be consistent with the initiation and propagation of micro cracks, and a reasonable damage variable must meet four basic requirements: (1) it has a distinct physical meaning; (2) it can be measured easily and applied conveniently in engineering; (3) its evolution law coincides well with the actual degradation process of material; (4) it can take the initial damage into account [35-37].

In this paper, porosity is selected as the key parameter to form the damage variable *D*, which is tested and obtained by using NMR system. A damage model is then developed using such damage variable. The micro damage variable can be calculated as [38]:

$$D = \frac{V - V_D}{V} = \frac{n - n_0}{1 - n_0} \qquad (1)$$

Where *D* is the damage variable, n_0 is the porosity of the intact sample, and n is the porosity of the sample after suffered external damage, such as chemical erosion or loads. The whole damage induced by chemical erosion coupled cyclic loads is assumed to exist simultaneously and independently, which can be expressed as:

$$D = D_c + D_m + zD_cD_m \qquad (2)$$

Where *D* is the whole damage of the test rock, D_c is the variable of chemical erosion damage, D_m is the mechanical damage variable induced by cyclic loads, z is the coupled damage variable, and D_cD_m is the coupled damage induced by cyclic loads and chemical erosion.

The damage of the rock induced by cyclic loads can be divided into low-cycle fatigue and high-cycle fatigue. Low-cycle fatigue means the rock can withstand less than 10^4 time of cyclic loads, while high-cycle fatigue means the rock can withstand over 10^4 time of cyclic loads, and there is no obvious plastic deformation or macro cracks occurs [18]. According to NMR and mechanical test results, the limestone in belongs to low-cycle fatigue ones. Thus, the damage development rate can be expressed as [39]:

$$D' = (\frac{Y}{Q})^q p \quad (3)$$

Where Y is the energy dissipation rate, p is the cumulative plastic strain rate, and q and Q are parameters.

D is the whole damage of the limestone samples in the one-dimensional condition, and the free energy density function, $\emptyset$, can be expressed as follows:

$$\emptyset = \frac{\sigma^2}{2pE(1-D)} + K \quad (4)$$

Where σ is the axial stress, p is the mass density, and K is an item unrelated to the rock damage. The energy dissipation rate for the damage can be expressed as follows:

$$Y = -p\frac{\partial \emptyset}{\partial D} = \frac{1}{2E}(\frac{\sigma}{1-D})^2 \quad (5)$$

When the rock is loaded, the equation for micro-plastic strain rate is as follows[40]:

$$\varepsilon' = p = f\frac{\sigma^{f-1}\sigma'}{F^f(1-D)^f(\partial\sigma)^a N^c} \quad (6)$$

Where F is loads, σ' is stress rate, N is the cycle times, f, a, c are parameters.

Based on formula (3), (5), (6), the following formula can be obtained as follows:

$$D' = \frac{\sigma^{b-1}\sigma'}{B(1-D)^b(\partial\sigma)^a N^c} \quad (7)$$

Where *a* and *B* are parameters, and b= f+ 2q, B = $(2EQ)^q F^f$/ f.

The damage rate D' is assumed to be small and approximately constant in each fatigue cycle. Moreover, the stress unloading is not considered to cause rock damage. Thus, when Eq. (12) is integrated into a complete stress loading and unloading cycle, the damage factor induced by cyclic loads can be expressed as follows:

$$\frac{\partial D}{\partial N} = 2\int_{\sigma_{min}}^{\sigma_{max}} \frac{\sigma^{b-1}\sigma'}{B(1-D)^b(\partial\sigma)^a N^c} = 2\frac{\sigma_{max}^b - \sigma_{min}^b}{bB(1-D)^b(\partial\sigma)^a N^c} \quad (8)$$

Where σ_{max} and σ_{min} is the maximum load and minimum load during the whole cyclic loading process.

For the rock under cyclic loading, the boundary condition can be:

When $N=0$, $D=0$, while $N=N_f$, $D=1$. $N_f = \left[\frac{bB}{2(b+1)(\sigma_{max}^{b}-\sigma_{min}^{b})}\right]^{\frac{1}{1-c}}$

So the damage factor of a rock subjected only to cyclic stress is as follows:

$$D_m = 1 - \left[1 - (\frac{N}{N_F})^{1-c}\right]^{\frac{1}{b+1}} \quad (9)$$

Eq. (9) has the same expression as the damage models proposed by Li et al. [41].

The limestone samples in this test are mainly composed of calcspar, which can easily react with acid ions (*e.g.* H^+), resulting an increase of the porosity. The following reactions are likely to occur in an acidic solution:

$$CaCO_3 + 2H^+ \rightarrow Ca^{2+} + H_2O + CO_2 \uparrow \quad (10)$$

The reactions of the calcspar can be expressed as follows [42]:

$$Rate = Ak(\Omega^m - 1)^n \quad (11)$$

$$\Omega = \frac{IAP}{K} \quad (12)$$

Where Rate is the reaction rate of the calcspar, A is the reaction area of the sample, k is the chemical reaction rate parameter, K is the corresponding equilibrium constant, Ω is the solution saturation index, m and n are parameters, and IAP is the is the normalized saturation ratio. It is found that the effect of IAP on the overall behaviour of the chemical reaction system was relatively small, although the same is not true for changes in the formulation of the growth rate [40].

The density of the calcspar inside the limestone sample can be expressed as:

$$\frac{\partial(1-\varphi)p_l}{\partial t} = -\nabla(p_l\varphi v) + p_c V_c Rate \quad (13)$$

The porosity increment caused by chemical erosion can be expressed as follows:

$$\frac{\partial n_c}{\partial t} = rV_c Rate \quad (14)$$

Where r is the chemical reaction equivalent parameter, V_c is the molar volume of the calcspar, t is the erosion time. Therefore, from equation (1) and (13), the micro damage due to chemical erosion can be calculated by:

$$D_c = \frac{n_t - n_0}{1-n_0} = \frac{\mathrm{n_c}}{1-\mathrm{n_0}} \quad (15)$$

Where n_t is the porosity of the sample after chemical erosion, n_0 is the porosity of the intact sample. Combining equations (1), (9) and (14), the micro damage of limestone induced by cyclic loads coupled with chemical erosion can be expressed as:

$$D = D_c + D_m + zD_cD_m = 1 - \left[1 - (\frac{N}{N_F})^{1-c}\right]^{\frac{1}{b+1}} + \frac{rV_c tRate}{1-n_0} + z\frac{rV_c tRate}{1-n_0}(1 - \left[1 - (\frac{N}{N_F})^{1-c}\right]^{\frac{1}{b+1}}) \quad (16)$$

According to [42], the parameters of the fatigue damage model, Equation (16) can be obtained by fitting with data of samples immersed in pH3 values solution, and are shown in Table 2.

Table 2 Parameters for the proposed model

reaction area/m^2 × g^{-1}	logK	*m*	*n*	molar volume of the calcspar/ g/mol
7.07×10^{-3}	10.34	1	1	100
k/mol×m^2×s^{-1}	Density of calcspar/kg×m^{-3}	c	$\frac{1}{b+1}$	z
$1.724\times 10^{-6.8}$	2650	0.114	0.001	91.839

4.2 Damage model

Considering the damaged part not subjected to external loads and the intact part subjected to external loads, Rabotnov [41] proposed a damage model in terms of damage variable *D*:

$$\sigma_a = \sigma_i(1 - D) \quad (16)$$

Where σ_a is the apparent stress and σ_i is the stress of the intact part. This model will be used as the based damage model in this study.

The stress–strain relationship of the intact part agrees with Hooke's law. In triaxial stress paths:

$$\sigma_{i1} = E\varepsilon_{i1} + 2v\sigma_{i3} \quad (17)$$

Where σ_{i1}, σ_{i1} is the maximum stress and the minimum stress of the rocks respectively, $\varepsilon_{i1}$is the axial strain, *E* is the elastic modulus, *v* is the Poisson ratio.

And the apparent strain in the damaged part and the strain in the intact part are in accordance with Lemaitre equivalent strain theory as follows:

$$\varepsilon_i = \varepsilon_a \quad (18)$$

Where ε_i is the intact strain, and ε_a is the apparent strain.

From Equation (16)-(18), we can have:

$$\sigma_1 = (1 - D)E\varepsilon_1 + 2v\sigma_3 \qquad (19)$$

When $\sigma_3 = 0$, Equation (19) can be used for uniaxial condition.

5 Discussions

5.1 Relationship between micro damage and peak strength degradation

After cyclic loading, the chemical corroded and the water soft samples are tested by Rock 600-50 test system under compression until completely ruptured. The peak strength of the corroded samples after treated with different numbers of cyclic loads is shown in Table 3. The stress–strain curves of limestone samples after different loading cycles are shown in Fig 9 (a), (b) and (c). Attention is focused on samples corroded by pH3 solution, because there is more significant degradation of mechanical properties occurring in this sample group. The stress–strain curves of the water soft sample are plotted in Fig 9 (d), (e) and (f) for comparisons.

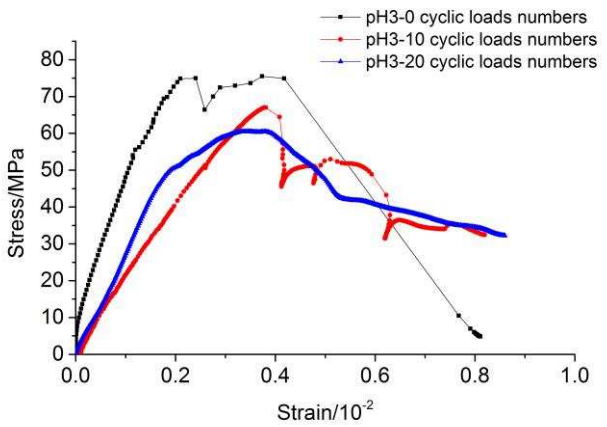

(a)

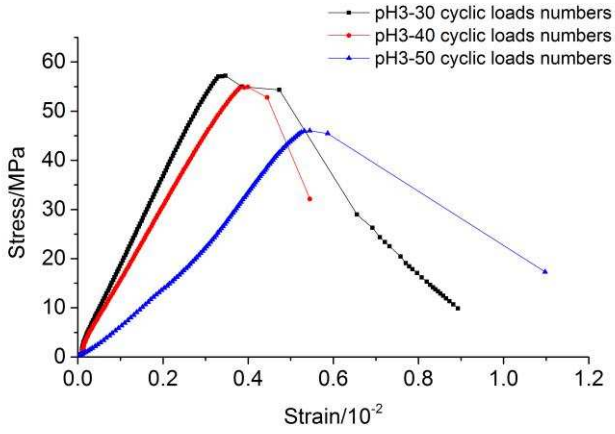

(b)

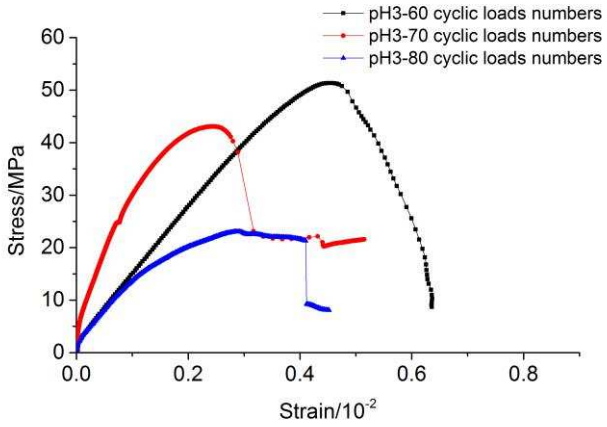

(c)

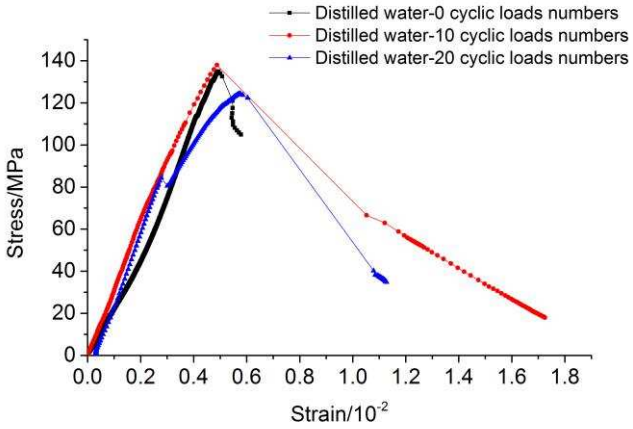

(d)

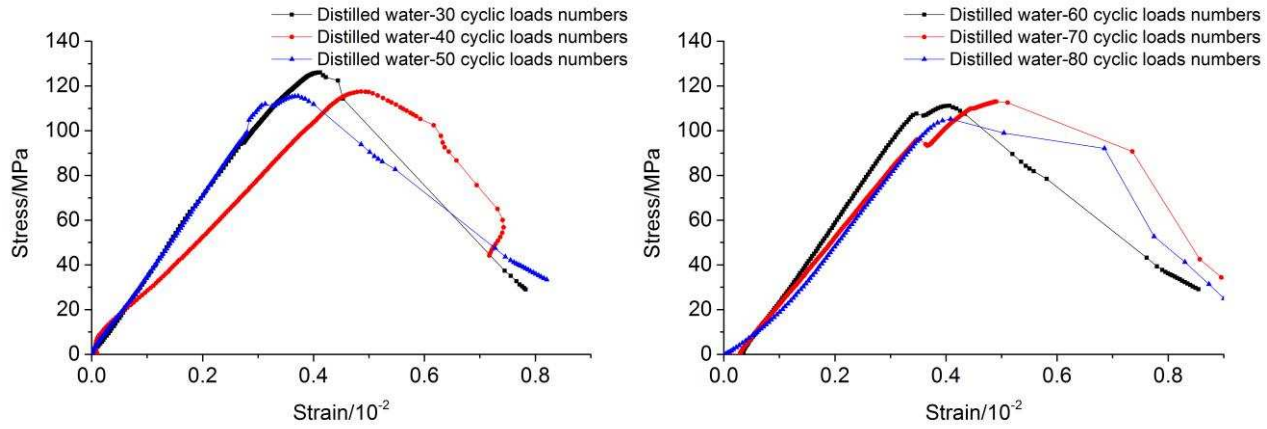

(e) (f)

Fig. 9 Stress–strain curves of limestone samples under compression.

Table 3 Peak strength of the corroded samples after cyclic loads (unit: MPa)

Samples' solution	Original peak strength	Peak strength after number of load cycles							
		10	20	30	40	50	60	70	80
pH3 Na2SO4	74.96	67.02	60.47	55.62	54.90	46.01	51.34	43.07	22.04
pH5 Na2SO4	101.35	95.68	86.18	84.43	82.85	77.98	80.05	76.50	70.64
pH7 Na2SO4	119.09	112.91	105.81	103.87	105.09	101.73	99.79	97.47	95.56
Distilled water	134.89	133.55	123.51	123.24	117.46	115.44	111.12	112.98	105.24

Peak strength of the limestone can be quantified by a strength degradation parameter (SDP), which can be defined as the following:

$$SDP = \frac{\sigma_i - \sigma_d}{\sigma_i} \qquad (20)$$

Where σ_i is the original peak strength which belongs to the intact limestone sample, and σ_d is the peak strength of the damaged sample.

Fig.10 shows the relationship between micro damage and SDP of limestone samples after cyclic loading, and the corresponding micro damage rates is calculated and shown in Table 4.

Table 4 Micro damage rates of the corroded samples after cyclic loads (unit: MPa)

	Micro damage rates after number of load cycles

Samples' solution	Original micro damage	10	20	30	40	50	60	70	80
pH3 Na_2SO_4	0.0230	0.0303	0.0333	0.0345	0.0353	0.0360	0.0371	0.040	0.0451
pH5 Na_2SO_4	0.0155	0.0218	0.0239	0.0249	0.0259	0.0264	0.0276	0.0297	0.0332
pH7 Na_2SO_4	0.0083	0.0138	0.0155	0.0165	0.0169	0.0177	0.0187	0.0199	0.0210
Distilled water	0.0027	0.0074	0.0089	0.0095	0.0098	0.0102	0.0106	0.0111	0.0115

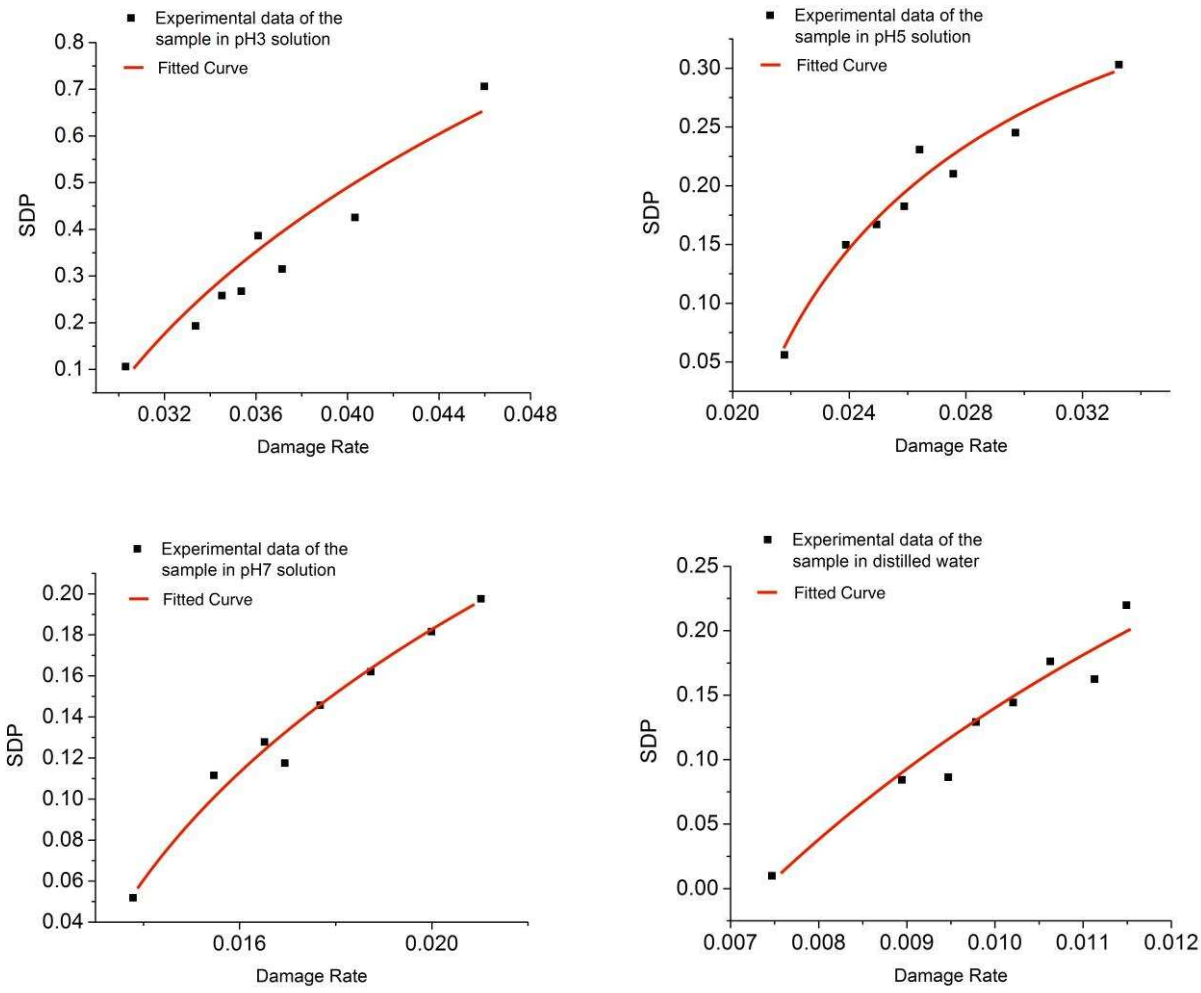

Fig.10 Strength degradation vs damage rate.

The observation from Fig.9, Fig.10, Table 3 and Table 4 is that: (1) SDP increases with the increasing micro damage rate, until it is approximately more than 4.5% at which point rock should be broken. (2) The chemical solutions have an impact on microstructure of limestone as well as the mechanical properties, and the cyclic fatigue affects the mechanical properties more seriously for the chemical corroded samples: with the same number of loading cycles, the peak strength of the chemical corroded samples is degraded much more significantly than that of the water soft ones.

This is because that the chemical solutions, such as Na_2SO_4, influence the mechanical properties of rock in two main ways [4-5]: (1) the chemical icons react with the mineral substance inside the limestone samples, weak the bridging bonds between the rock elements or close to crack tips, thus decrease the strength of the rock and facilitate micro crack growth and convergence at relative lower stress levels than would otherwise be the case. (2) Under cyclic loading, the stresses are continuously redistributed in the rock and the fracture toughness decreases allowing more subcritical crack to grow which consequently leads to stress corrosion and mechanical properties degradation. Moreover, the chemical erosion weakens the structure and cementing capability of the limestone samples, therefore micro flaws or cracks would propagate and grow quickly under cyclic loading.

5.2 Micro damage evolution law

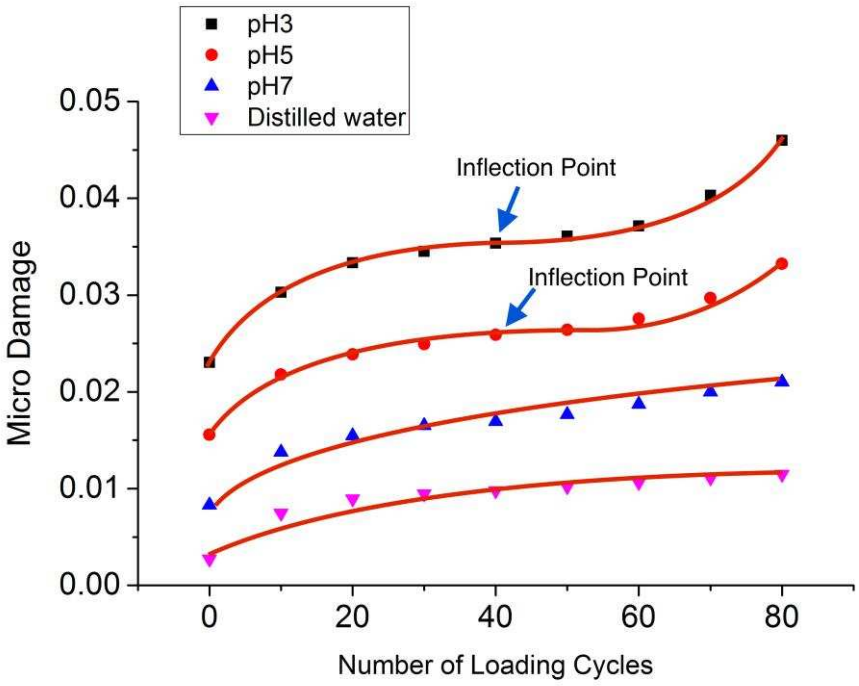

Fig. 11 Micro damage vs number of loading cycles

The damage rate evolution law of all the samples is shown in Fig 11. As it is talked in Chapter 3.1, there are three damage evolution stages of the corroded sample treated with cyclic loads: micro crack emergence stage, micro damage development stage and damage acceleration stage. These stages are also plotted in Fig 11.

Combined with NMR test results, Fig 6 and Fig 7, it can be found that: (1) When the loading cycle is low (taking samples corroded by pH3 solution as an example), around 20 cycles, the damage evolution curve is obviously convex. Then the micro damage rise steadily with the increasing loading cycles. After 60 loading cycles, the damage evolution curve becomes concave. The inflection point in the micro damage-loading cycles curve is plotted (see Fig. 10).

(2) The inflection point in the micro damage-loading cycles curve is a turning point of the micro damage evolution process: before this point, the main change of the T_2 spectrum curves takes place in the first and second peaks, which indicates the micro damage of limestone in this stage is caused by sharp increase in number and size of micro cracks. While after this point, the third peak of the T_2 spectrum curve increases rapidly, which indicates the micro cracks increasing is restrained, the micro damage of limestone is caused by micro crack connection.

(3) The inflection point in the damage curve of the chemical corroded sample often emerge in lower loading cycles compared to others, so that the ultimate loading cycles (until the sample rupture) of the chemical corroded samples, is shorter than water soft ones. This is because after chemical erosion, the rock structure of limestone samples becomes softer, that accelerates the convergence of the micro crack as well as the rupture stage, and makes the damage evolution process become faster.

6 Conclusions

In this study NMR technique has been used to investigate the micro damage evolution of limestone under chemical erosion coupled with cyclic loading. Based on the experimental results, some conclusions can be drawn as below:

(1) By using NMR system, T_2 spectrum curves and MRI of porosity are obtained. The micro damage of the chemical corroded rock under cyclic loading is visualized. The results shed a light to better understanding of micro damage evolution law and the microscopic mechanical behaviour of the sedimentary rocks, limestone, via a non-destructive approach.

(2) According to MRI and T_2 spectrum curves, the porosity and micro cracking of the corroded limestone samples increase with the cyclic loading, and the micro damage development process has shown three stages: micro crack compaction and emergence stage, micro damages development stage and damage develop accelerated stage.

(3) There is a close relationship between chemical erosion and the micro damage developments: micro damage, which includes the porosity and micro cracking, of the chemical corroded samples under cyclic loading often develop faster than the water softened ones. The damage development stage of the chemical corroded samples often shorter and less obvious compared to the water soft ones.

(4) The inflection point in the micro damage-loading cycles curve is a turning point of the micro damage evolution process: before this point, the main damage of the corroded sample under cyclic loads is caused by new micro cracks increase inside the limestone; while after this point, the new micro crack emergence is being restrained, and the existed micro cracks connect into rupture bond.

(5) After cyclic loading, the chemical corroded samples always have lower peak strength compared with the water soft ones.

(6) Based on experimental data, a micro damage model is established to qualify the damage evolution for the chemical corroded limestone under cyclic loading. The proposed damage model will be useful for predicting rock strength in the design of underground constructions, slops and dams and roads in water surrounded regions.

Reference

[1]CHOI, S. R., NEMETH, N. N. & GYEKENYESI, J. P. Slow crack growth of brittle materials with exponential crack velocity under cyclic fatigue loading[J]. International Journal of Fatigue. 2006, 28(2):164-172.

[2]MUNOZ, H. & TAHERI, A. Local Damage and Progressive Localisation in Porous Sandstone During Cyclic Loading[J]. Rock Mechanics and Rock Engineering. 2017:1-7.

[3]MARTIN, C., KAISER, P. & CHRISTIANSSON, R. Stress, instability and design of underground excavations[J]. International Journal of Rock Mechanics and Mining Sciences. 2003, 40(7):1027-1047.

[4]HU, D., ZHOU, H., HU, Q., SHAO, J., FENG, X. & XIAO, H. A hydro-mechanical-chemical coupling model for geomaterial with both mechanical and chemical damages considered[J]. Acta Mechanica Solida Sinica. 2012, 25(4):361-376.

[5]SETO, M., NAG, D. K., VUTUKURI, V. S. & KATSUYAMA, K. Effect of chemical additives on the strength of sandstone[J]. International Journal of Rock Mechanics and Mining Sciences. 1997, 34(3):280.e1-280.e11.

[6]BEN ABDELGHANI, F., AUBERTIN, M., SIMON, R. & THERRIEN, R. Numerical simulations of water flow and contaminants transport near mining wastes disposed in a fractured rock mass[J]. International Journal of Mining Science and Technology. 2015, 25(1):37-45.

[7]DEHKHODA, S. & HOOD, M. The internal failure of rock samples subjected to pulsed water jet impacts[J]. International Journal of Rock Mechanics and Mining Sciences. 2014, 66:91-96.

[8]LIU, X. S., NING, J. G., TAN, Y. L. & GU, Q. H. Damage constitutive model based on energy dissipation for intact rock subjected to cyclic loading[J]. International Journal of Rock Mechanics and Mining Sciences. 2016, 85(Supplement C):27-32.

[9]AL-SHAYEA, N. A. Effects of testing methods and conditions on the elastic properties of limestone rock[J]. Engineering Geology. 2004, 74(1):139-156.

[10]RAY, S. K., SARKAR, M. & SINGH, T. N. Effect of cyclic loading and strain rate on the mechanical behaviour of sandstone[J]. International Journal of Rock Mechanics and Mining Sciences. 1999, 36(4):543-549.

[11]YOSHINAKA, R., OSADA, M. & TRAN, T. V. Deformation behaviour of soft rocks during consolidated-undrained cyclic triaxial testing[J]. International Journal of Rock Mechanics and Mining Sciences & Geomechanics Abstracts. 1996, 33(6):557-572.

[12]YOSHINAKA, R., TRAN, T. V. & OSADA, M. Pore pressure changes and strength mobilization of soft rocks in consolidated-undrained cyclic loading triaxial tests[J]. International Journal of Rock Mechanics and Mining Sciences. 1997, 34(5):715-726.

[13]YOSHINAKA, R., TRAN, T. V. & OSADA, M. Non-linear, stress- and strain-dependent behavior of soft rocks under cyclic triaxial conditions[J]. International Journal of Rock Mechanics and Mining Sciences. 1998, 35(7):941-955.

[14]BAGDE, M. N. & PETROŠ, V. Fatigue and dynamic energy behaviour of rock subjected to cyclical loading[J]. International Journal of Rock Mechanics and Mining Sciences. 2009, 46(1):200-209.
[15]BAGDE, M. N. & PETROŠ, V. Fatigue properties of intact sandstone samples subjected to dynamic uniaxial cyclical loading[J]. International Journal of Rock Mechanics and Mining Sciences. 2005, 42(2):237-250.
[16]SUN, B., ZHU, Z., SHI, C. & LUO, Z. Dynamic mechanical behavior and fatigue damage evolution of sandstone under cyclic loading[J]. International Journal of Rock Mechanics and Mining Sciences. 2017, 94(Supplement C):82-89.
[17]LI, N., ZHANG, P., CHEN, Y. & SWOBODA, G. Fatigue properties of cracked, saturated and frozen sandstone samples under cyclic loading[J]. International Journal of Rock Mechanics and Mining Sciences. 2003, 40(1):145-150.
[18]ZHOU, S. W., XIA, C. C., HU, Y. S., ZHOU, Y. & ZHANG, P. Y. Damage modeling of basaltic rock subjected to cyclic temperature and uniaxial stress[J]. International Journal of Rock Mechanics and Mining Sciences. 2015, 77(Supplement C):163-173.
[19]MAHMUTOGLU, Y. Mechanical behaviour of cyclically heated fine grained rock[J]. Rock Mechanics and Rock Engineering. 1998, 31(3):169-179.
[20]HAZZARD, J. F., YOUNG, R. P. & MAXWELL, S. Micromechanical modeling of cracking and failure in brittle rocks[J]. Journal of Geophysical Research: Solid Earth. 2000, 105(B7):16683-16697.
[21]KEMENY, J. M. Micromechanics of deformation in rocks[J]. Quasi-BrittleMaterials. 1990:167.
[22]KRANZ, R. L. Crack-crack and crack-pore interactions in stressed granite[J]. International Journal of Rock Mechanics and Mining Sciences & Geomechanics Abstracts. 1979, 16(1):37-47.
[23]FENG, X. T., CHEN, S. L. & ZHOU, H. Real-time computerized tomography (CT) experiments on sandstone damage evolution during triaxial compression with chemical corrosion[J]. International Journal of Rock Mechanics and Mining Sciences. 2004, 41(2):181-192.
[24]KAWAKATA, H., CHO, A., KIYAMA, T., YANAGIDANI, T., KUSUNOSE, K. & SHIMADA, M. Three-dimensional observations of faulting process in Westerly granite under uniaxial and triaxial conditions by X-ray CT scan[J]. Tectonophysics. 1999, 313(3):293-305.
[25]LI, S., ZHOU, Z., LI, X., LIU, L., HE, J. & LIU, Y. One CT imaging method of fracture intervention in rock hydraulic fracturing test[J]. Journal of Petroleum Science and Engineering. 2017, 156:582-588.
[26]SATO, A. & OBARA, Y. Analysis of Pore Structure and Water Permeation Property of a Shale Rock by Means of X-Ray CT[J]. Procedia Engineering. 2017, 191:666-673.
[27]RAMIA, M. & MARTÍN, C. Sedimentary rock porosity studied by electromagnetic techniques: nuclear magnetic resonance and dielectric permittivity[J]. Applied Physics A. 2015, 118(2):769-777.
[28]SØRLAND, G. H., DJURHUUS, K., WIDERØE, H. C., LIEN, J. R. & SKAUGE, A. Absolute pore size distributions from NMR[J]. Diffusion Fundamentals. 2007, 5:4.1-4.15.
[29]WEBBER, J. B. W., CORBETT, P., SEMPLE, K. T., OGBONNAYA, U., TEEL, W. S., MASIELLO, C. A., FISHER, Q. J., VALENZA, J. J., SONG, Y.-Q. & HU, Q. An NMR study of porous rock and biochar containing organic material[J]. Microporous and Mesoporous Materials. 2013, 178:94-98.
[30]ZHOU, K.-P., BIN, L., LI, J.-L., DENG, H.-W. & FENG, B. Microscopic damage and dynamic mechanical properties of rock under freeze–thaw environment[J]. Transactions of Nonferrous Metals Society of China. 2015, 25(4):1254-1261.
[31]LIU, H., D'EURYDICE, M. N., OBRUCHKOV, S. & GALVOSAS, P. Determining pore length scales and pore surface relaxivity of rock cores by internal magnetic fields modulation at 2MHz NMR[J]. Journal of Magnetic Resonance. 2014, 246:110-118.

[32]LUO, S., XU, R., JIANG, P. & HUANG, X. Visualization experimental investigations of supercritical CO2 inject into porous media with the fissure defect[J]. Energy Procedia. 2011, 4:4411-4417.
[33]CHANG, C., ZOBACK, M. D. & KHAKSAR, A. Empirical relations between rock strength and physical properties in sedimentary rocks[J]. Journal of Petroleum Science and Engineering. 2006, 51(3):223-237.
[34]XIAO, J.-Q., DING, D.-X., JIANG, F.-L. & XU, G. Fatigue damage variable and evolution of rock subjected to cyclic loading[J]. International Journal of Rock Mechanics and Mining Sciences. 2010, 47(3):461-468.
[35]EBERHARDT, E., STEAD, D. & STIMPSON, B. Quantifying progressive pre-peak brittle fracture damage in rock during uniaxial compression[J]. International Journal of Rock Mechanics and Mining Sciences. 1999, 36(3):361-380.
[36]FAN, X.-F., WU, Z.-X. & JIAN, W.-B. Analysis of acoustic property of sandstone fatigue damage under cyclic loading[J]. Rock and Soil Mechanics. 2009, 30(S1):58-62.
[37]MARTIN, C. & CHANDLER, N. The progressive fracture of Lac du Bonnet granite. International Journal of Rock Mechanics and Mining Sciences & Geomechanics Abstracts, 1994. Elsevier, 643-659.
[38]KACHANOV, L. M. Rupture time under creep conditions[J]. International journal of fracture. 1999, 97(1-4):11-18.
[39]LEMAITRE, J. & DESMORAT, R. 2005. Engineering damage mechanics: ductile, creep, fatigue and brittle failures, Springer Science & Business Media.
[40]ATTEWELL, P. B. & FARMER, I. W. Fatigue behaviour of rock[J]. International Journal of Rock Mechanics and Mining Sciences & Geomechanics Abstracts. 1973, 10(1):1-9.
[41]LI, S. C., XU, J., TAO, Y. Q., TANG, X. J. & YANG, H. W. 2009. Low cycle fatigue damage model and damage variable expression of rock.
[42]STEEFEL, C. I. & VAN CAPPELLEN, P. A new kinetic approach to modeling water-rock interaction: The role of nucleation, precursors, and Ostwald ripening[J]. Geochimica et Cosmochimica Acta. 1990, 54(10):2657-2677.